Simulations and Design of Microfabricated Interdigitated Electrodes for Use in a Gold Nanoparticle Enhanced Biosensor*

Peter Hermansen, Scott MacKay, David Wishart, and Jie Chen

Abstract— **Microfabricated interdigitated electrode chips have been designed for use in a unique gold-nanoparticle based biosensor system. The use of these electrodes will allow for simple, accurate, inexpensive, and portable biosensing, with potential applications in diagnostics, medical research, and environmental testing. To determine the optimal design for these electrodes, finite element analysis simulations were carried out using COMSOL Multiphysics software. The results of these simulations determined some of the optimal design parameters for microfabricating interdigitated electrodes as well as predicting the effects of different electrode materials. Finally, based on the results of these simulations two different kinds of interdigitated electrode chips were made using photolithography.**

I. Introduction

Microfabrication allows for interfacing fabricated components directly with biological and chemical elements in new ways, creating opportunities for new devices. One example of this is biosensor devices. In the most general sense, a biosensor is a device which can detect, measure and report the presence of specific components in biological samples, with one of the most common examples of a biosensor being glucose sensors used by people to monitor and control diabetes [1], [2]. By detecting different biological components, biosensors can be used for numerous applications in healthcare and diagnostics. Many of these devices can take advantage of microfabricated components to allow for accurate and sensitive detection of components in biological samples [3]. Some examples of these include microfabricated cantilevers which bend under the weight of bound specific biomolecules [3], [4], and microfabricated electrodes which can be used for electrical detection of biomolecules [5], [6]. Though designs of biosensor electrodes can vary, one popular design is using interdigitated electrodes (IDEs) [7]–[9]. Essentially just microfabricated capacitors, IDEs consist of two conducting comb electrodes with interlocking digits, shown in Fig 1. The dimensions and materials of microfabricated IDEs for biosensors can vary depending on the exact application. Electrodes with larger dimensions and space between electrode digits (in the range of 10's of microns) can be appropriate for detecting cells growing on the electrodes [8], [10], [11], whereas much smaller dimensions (several microns or below) are required for detecting small molecules such as DNA [7], [9].

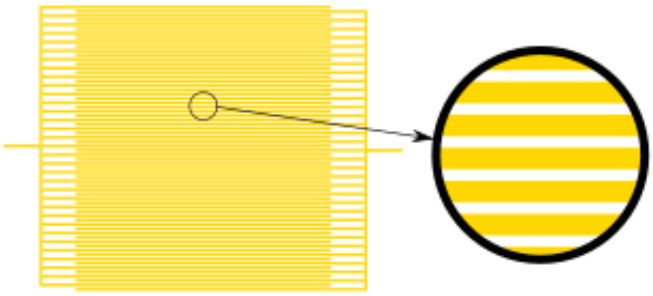

Figure 1. Basic structure of an interdigitated electrode.

This paper outlines the design of IDEs for use in a handheld impedance-based biosensor system. Detection in this system is based on binding gold nanoparticles in between IDE digits to induce a change in the measured electrical impedance of the electrodes (shown in Fig 2). The proposed mechanism is based on binding molecular recognition elements (MREs) such as antibodies or binding proteins between electrode digits. MREs bind specifically to a particular biomolecule (in this case the biomolecule detected by that sensor), this binding is then designed to facilitate the binding of a modified gold nanoparticle to the biomolecule/MRE complex. Thus the presence of the target biomolecule leads to bound nanoparticles between the electrodes, leading to a measurable change in impedance.

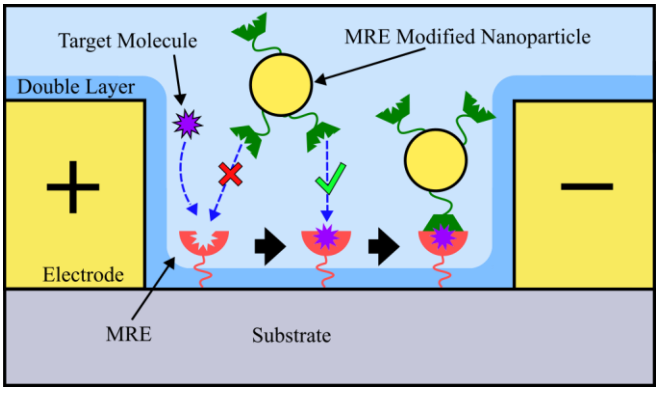

Figure 2. Detection mechanism of the biosensor system. MREs are bound between adjacent digits on the IDE. The binding of the target biomolecule causes modified gold nanoparticles to bind to the surface and modify the impedance spectrum of the electrodes.

*This work was supported by the Canadian National Research Council/National Institute for Nanotechnology (NRC/NINT), Natural Sciences and Engineering Research Council of Canada (NSERC), and Alberta Innovates- Health Solutions (AIHS), Alberta Innovates – Technology Futures (AITF)

Peter Hermansen is with the Electrical and Computer Engineering Department, University of Alberta, Canada (email: phermans@ualberta.ca).

Scott MacKay is with Electrical and Computer Engineering Department, University of Alberta, Canada (e-mail: samackay@ualberta.ca).

David Wishart is with Biological Sciences Department and Computing Science Department, University of Alberta, Canada. He is also affiliated with National Research Council/National Institute for Nanotechnology, Canada (e-mail: david.wishart@ualberta.ca).

Jie Chen is with Electrical and Computer Engineering Department, Biomedical Engineering Department, University of Alberta, Canada. He is also affiliated with National Research Council/National Institute for Nanotechnology, Canada (e-mail: jc65@ualberta.ca).

978-1-4577-0220-4/16/$31.00 ©2016 IEEE

In order to design the appropriate IDEs for this application, simulations were carried out to determine the ideal dimensions and conditions for this biosensor. These simulations were set up to test factors such as the ideal dimensions of the electrodes, the effect of bound nanoparticles on the electrodes, and the best electrode materials. Next, based in part on these simulation results, electrodes were fabricated using standard photolithographic microfabrication techniques.

II. Simulations

To perform finite element method simulations COMSOL Multiphysics software was used. This allowed for identification of frequency ranges and electrode dimensions that are more sensitive to bound gold nanoparticles. Simulations were run on different electrode geometric parameters in order to optimize the IDE design for electrochemical impedance spectroscopy (EIS). In order to simplify the simulations a 2D setup was used. Due to the symmetry of the electrode setup, impedance results from the 2D setup can be used to calculate the 3D setup as follows:

$$Z = \frac{v_{app}}{(N_e - 1)L_e\sqrt{J_x^2 + J_y^2}}. \quad (1)$$

Where N_e is the total number of electrode digits, L_e is the length of the electrodes, J_x and J_y are the current densities in the simulated plane, and v_{app} is the applied voltage. An assumption made by this set up is that the electrodes only interact with their nearest pair. The difference in impedance when simulations with multiple electrodes were run compared to when only a single pair was run were negligible. In order for the system of achieve linear behavior the applied voltage was chosen to be less than the thermal voltage (about 25mV) [12]. To model the double layer the sterically modified Poisson-Boltzmann model is used. Where differential capacitance can be described for single valence ions as [13]:

$$C = \frac{\epsilon}{4\pi\lambda_D}\cosh\left(\frac{\phi_0}{2}\right)\frac{\sqrt{2}\left|\sinh\frac{\phi_0}{2}\right|}{\cosh\phi_0\sqrt{\ln(\cosh\phi_0)}}. \quad (2)$$

Here ϵ is the permittivity, λ_D is the Debye length, and $\phi_0 = \frac{e\Phi}{k_B T}$ where Φ is the electrostatic potential.

The height of all simulated electrode systems was 50nm. This was chosen because it is the standard thickness of deposited layers in the photolithography process used. A range of digit gap sizes and ratios of digit width to gap size were simulated from 1 to 100MHz for gold electrodes fabricated on borosilicate glass. This allows for comparison of different geometric properties as well as identification of the frequency ranges which provide optimal sensitivity. The sensitivity was evaluated by comparing the impedance spectrum with and without gold nanoparticles. The gold nanoparticles had a radius of 30nm which was chosen based on commercial availability and were simulated such that they covered 10% of the area between electrodes. The sensitivity value was dependent on the location of gold nanoparticles in the gap so a wide range of gold nanoparticle positions were simulated for each frequency and the resulting sensitivities were averaged. The sensitivity is calculated as:

$$S = \frac{|Z_{no\ GNPs} - Z_{GNPs}|}{Z_{no\ GNPs}} * 100 \quad (3)$$

The peak sensitivities of a range of gap sizes and the cutoff frequencies representing the optimal measurement range value are plotted in Fig. 3, keeping the ratio of gap to electrode size at 1:2. Similarly plots for a range of electrode to gap size ratios are plotted keeping the gap size at 2µm in Fig. 4.

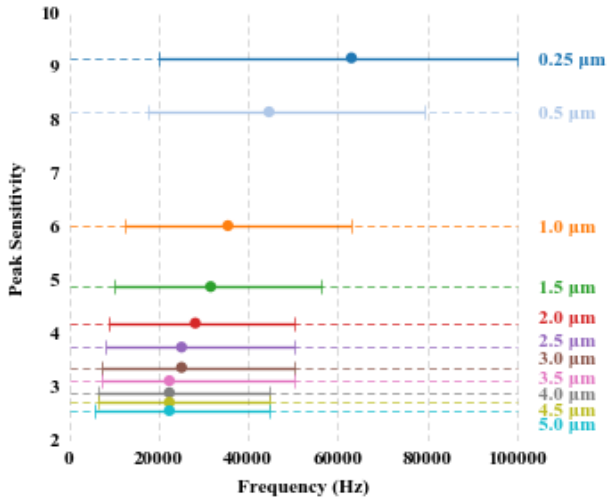

Figure 3. Peak sensitivity values and cutoff frequencies of different gap sizes with electrodes kept at a 1:2 gap to digit ratio.

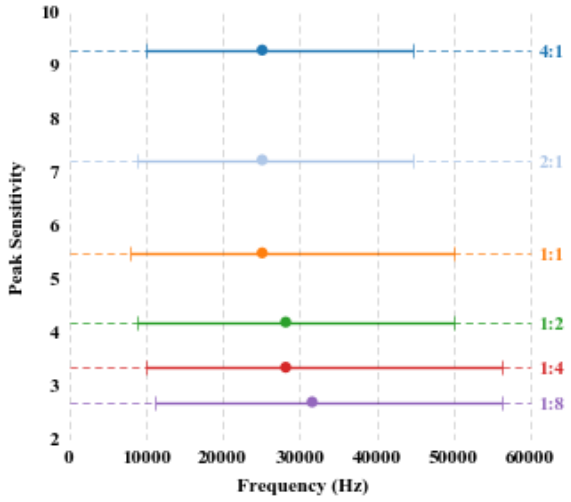

Figure 4. Peak sensitivity values and cutoff frequencies of different gap to digit ratios with electrodes kept at a 2µm gap size.

As can be seen from these figures reducing the gap size between digits and reducing the electrode digit width relative to the gap size both result in increases in sensitivity.

However both the peak sensitivity value and the size of the ideal frequency measurement range increases with a decrease in gap size, and decreases with a reduction in the electrode digit width relative to the gap size. The reason why the location of the ideal test frequencies is important is because electronic systems capable of measuring the impedance spectrum of the electrodes would be easier to implement with greater accuracy if the measurement frequencies are lower and restricted to a smaller range. For this reason reduction of gap size to digit size ratios, either alone or in tandem with reduction in the electrode gap size would provide optimal sensitivity. The cost per electrode and electrode yield needs to be accounted for as well. As a result when selecting dimensions for fabricating electrodes the smallest dimensions that can be achieved with standard photolithography techniques, and minimal defects was chosen.

In addition to this simulations were performed for aluminum electrodes with a 1nm aluminum oxide layer fabricated on a silicon wafer with a 0.5µm thermally grown oxide layer. This was simulated with a 2µm digit gap, a 1:2 gap to digit ratio, and 10% gold nanoparticle area coverage in the gap. Although gold is commonly used as a material due to biocompatibility [14] aluminum on silicon would be less expensive to fabricate and an aluminum oxide layer is formed that can prevent degradation of the electrodes. The impedance magnitudes and phases of the two different electrodes are plotted in Fig. 5. Fig. 6 compares the sensitivities over a range of frequencies between these two electrodes. As can be seen the aluminum electrodes are marginally less sensitive than the gold having a peak value of 3.74% and 4.26%.

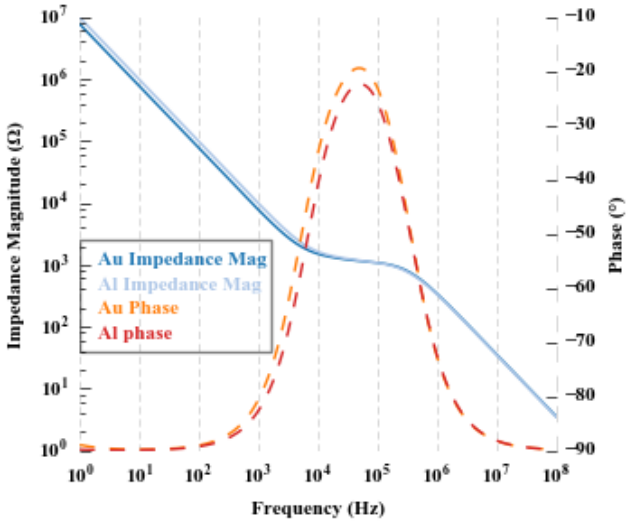

Figure 5. Impedance magnitude and phase of aluminum and gold electrodes with a 2µm gap and 1:2 gap to digit ratio.

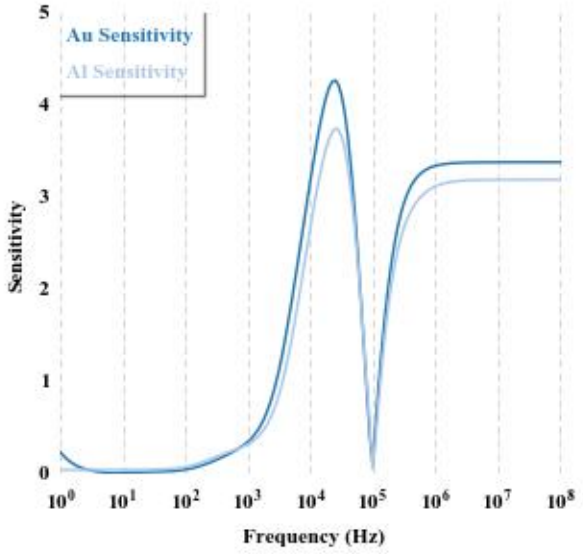

Figure 6. Comparison of the sensitivity of gold and aluminum electrodes to bound gold nanoparticles over a range of measurement frequencies.

III. Electrode Fabrication

Based on these COMSOL simulations, particularly those comparing electrode spacing, a photomask was made for making IDE chips using photolithography. The mask pattern has six "electrode chips" with eight separate IDEs on each chip. Based on the simulations, an electrode digit width of 4µm was chosen with a gap spacing of 2µm. Simulations show that this size should be sufficient for high sensitivity detection of gold nanoparticles. While smaller dimensions should result in more sensitivity, dimensions were kept large enough for standard photolithographic techniques to reduce the cost per electrode and the number of defects. Using the mask, electrodes were made using standard photolithography, sputtering, and wet etching. Two variations of the chips were made. The first were 50nm thick aluminum electrodes (which naturally form a thin aluminum oxide layer on them) patterned on silicon dioxide grown on silicon wafers, shown in Fig. 7. The second were 50nm thick gold electrodes patterned on borosilicate glass (with a chromium adhesion layer).

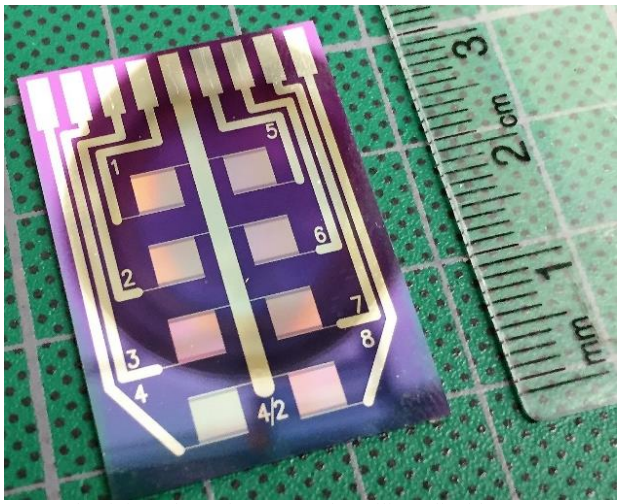

Figure 7. Aluminium electrodes patterned on silicon dioxide

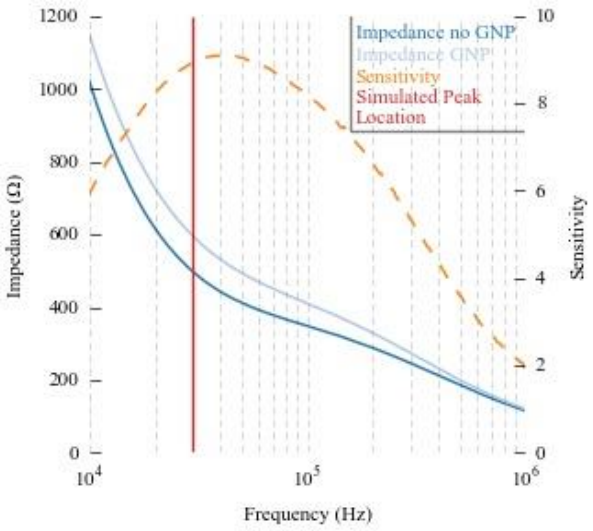

Figure 8. Preliminary experimental results showing impedance magnitude with and without GNPs, the calculated sensitivity and the location of the simulated sensitivity peak from Fig. 3.

Preliminary experiments were run to test the proposed detection mechanism. Here gold nanoparticles were directly chemically bound between the electrodes without the presence of a target molecule. Aluminum electrodes were used as opposed to the gold because the aluminum had fewer defects from fabrication. To perform EIS a Biologic SP-200 potentiostat was used. Early results show that the form of the EIS curve is very similar to simulated, but is shifted to slightly to higher frequencies. This is apparent in Fig. 8 depicting a range of measured frequencies and the calculated sensitivity. Here the location of the simulated peak is depicted by a red line. As can be seen the actual peak lies at a higher frequency. It should be noted that the value of the measured peak sensitivity is higher than the simulated peak value. This is likely because the surface coverage of gold nanoparticles is greater in the experimental results than the 10% simulated.

IV. Conclusion

Interdigitated electrode chips were designed and fabricated based on the results of simulations of their effectiveness in an impedance-based biosensor system. Since the IDEs used for this biosensor are fabricated using photolithography, testing many different types of electrodes with different dimensions would be incredibly time-consuming and expensive. The purpose of these simulations was to test the effectiveness of a wide range of different conditions as to narrow down the design for the fabricated electrodes. Conditions such as ranges of electrode dimensions, electrode material, and impedance measurement frequency were simulated for their effect on electrode sensitivity to gold nanoparticles. These simulations showed that in general smaller electrode gaps and a higher digit to gap ratio for the electrodes results in more sensitive detection. Additionally, simulations showed only a small difference in performance between gold and aluminum electrodes. Based on these simulations, gold and aluminum electrodes were made using photolithography.

Future work will focus on more characterization and measuring the fabricated electrodes. Impedance spectroscopy will be used to measure the impedance of different electrodes over a range of frequencies and then compare these results to the simulations. The effectiveness of the aluminum and gold electrodes will be compared in relation to their sensitivity and reliability. The effect of gold nanoparticles on the electrodes will be tested, and compared to the simulations.

Acknowledgment

We would like to thank the University of Alberta Nanofab staff for help with the fabrication of electrode chips, and Abebaw Jemere and Zhimin Yan.

References

[1] E. Yoo and S. Lee, “Glucose biosensors: An overview of use in clinical practice,” *Sensors*, vol. 10, pp. 4558–4576, 2010.

[2] J. Wang, “Glucose biosensors: 40 years of advances and challenges,” *Electroanalysis*, vol. 13, no. 12, pp. 983–988, 2001.

[3] A. Hierlemann and O. Brand, “Microfabrication techniques for chemical/biosensors,” *Proc. IEEE*, vol. 91, no. 6, pp. 839–863, 2003.

[4] C. Savran and S. Knudsen, “Micromechanical detection of proteins using aptamer-based receptor molecules,” *Anal. Chem.*, vol. 76, no. 11, pp. 3194–3198, 2004.

[5] M. Moreno, V. M. González, E. Rincón, a Domingo, and E. Domínguez, “Aptasensor based on the selective electrodeposition of protein-linked gold nanoparticles on screen-printed electrodes.,” *Analyst*, vol. 136, no. 9, pp. 1810–5, May 2011.

[6] B. Jang and A. Hassibi, “Biosensor systems in standard CMOS processes: fact or fiction?,” *Ind. Electron. IEEE Trans.*, vol. 56, no. 4, pp. 979–985, 2009.

[7] A. Bonanni, I. Fernández-Cuesta, X. Borrisé, F. Pérez-Murano, S. Alegret, and M. Valle, “DNA hybridization detection by electrochemical impedance spectroscopy using interdigitated gold nanoelectrodes,” *Microchim. Acta*, vol. 170, pp. 275–281, Apr. 2010.

[8] R. Ehret, W. Baumann, M. Brischwein, a Schwinde, and B. Wolf, “On-line control of cellular adhesion with impedance measurements using interdigitated electrode structures.,” *Med. Biol. Eng. Comput.*, vol. 36, no. 3, pp. 365–70, May 1998.

[9] J. Ahn, T. H. Lee, T. Li, K. Heo, S. Hong, J. Ko, Y. Kim, Y.-B. Shin, and M.-G. Kim, “Electrical immunosensor based on a submicron-gap interdigitated electrode and gold enhancement.,” *Biosens. Bioelectron.*, vol. 26, no. 12, pp. 4690–6, Aug. 2011.

[10] R. Ehret, W. Baumann, M. Brischwein, a Schwinde, K. Stegbauer, and B. Wolf, “Monitoring of cellular behaviour by impedance measurements on interdigitated electrode structures.,” *Biosens. Bioelectron.*, vol. 12, no. 1, pp. 29–41, Jan. 1997.

[11] S. Radke and E. Alocilja, “Design and fabrication of a microimpedance biosensor for bacterial detection,” *Sensors Journal, IEEE*, vol. 4, no. 4, pp. 434–440, 2004.

[12] G. Barbero, a. L. Alexe-Ionescu, and I. Lelidis, “Significance of small voltage in impedance spectroscopy measurements on electrolytic cells,” *J. Appl. Phys.*, vol. 98, no. 11, 2005.

[13] A. a Kornyshev, “Double-Layer in Ionic Liquids: Paradigm Change?,” *J. Phys. Chem. B*, vol. 111, no. 20, pp. 5545–5557, 2007.

[14] A. Manickam, A. Chevalier, M. McDermott, A. D. Ellington, and A. Hassibi, “A CMOS Electrochemical Impedance Spectroscopy (EIS) Biosensor Array.,” *IEEE Trans. Biomed. Circuits Syst.*, vol. 4, no. 6, pp. 379–90, Dec. 2010.